DMD Fast Forward. Published on August 25, 2006 as doi:10.1124/dmd.106.010991
This article has not been copyedited and formatted. The final version may differ from this version.

DMD #10991

# Functional analysis of Mouse and Monkey Multidrug resistance-associated protein 2 (Mrp2)

Mizuki Ninomiya, Kousei Ito, Remi Hiramatsu, and Toshiharu Horie

Laboratory of Biopharmaceutics, Graduate school of Pharmaceutical Sciences, Chiba University (M.N., R.H., T.H.), Department of Pharmacy, The University of Tokyo Hospital, The University of Tokyo (K.I.)

DMD Fast Forward. Published on August 25, 2006 as DOI: 10.1124/dmd.106.010991
This article has not been copyedited and formatted. The final version may differ from this version.



**Running title:**

Mouse and Monkey Mrp2 expressed in Sf9 cells

**The corresponding author:**

Toshiharu Horie, Ph.D., Professor, Laboratory of Biopharmaceutics, Graduate School of Pharmaceutical Sciences, Chiba University, Inohana 1-8-1, Chuo-ku, Chiba, 260-8675, Japan. Tel: 81-43-226-2886; Fax: 81-43-226-2886;

E-mail: horieto@p.chiba-u.ac.jp

**Text: 33 pages**

**The number of tables: 1**

**The number of figures: 6**

**The number of references: 46**

**Abstract: 218 words**

**Introduction: 642 words**

**Discussion: 1,366 words**

**Abbreviations:**

Mrp, multidrug resistance-associated protein; ABCC, ATP-binding cassette; transporter family C; TM, transmembrane; NBD, nucleotide binding domain; GSH, glutathione; $LTC_4$, leukotriene $C_4$; $E_2$17βG, 17β-estradiol 17-(β-D-glucuronide); EHBR, Eisai hyperbilirubinemic rats; HEK, human

embryonic kidney; MDCK, Mardin-Darby Canine Kidney; CCK-8, cholecystokinin octapeptide; BSP, bromosulfophthalein, 4-MUG, 4-methylumbelliferyl-β-D-glucuronide; PCR, polymerase chain reaction; MBP, maltose binding protein; PAGE, polyacrylamine gel electrophoresis; BSA, bovine serum albumin; TTBS, Tris-buffered saline with 0.05 % Tween 20; GFP, green fluorescent protein; $PS_{ns}$, non-saturable component; CMV, canalicular membrane vesicle; IM, indomethacin; TC, taurocholate

DMD Fast Forward. Published on August 25, 2006 as DOI: 10.1124/dmd.106.010991
This article has not been copyedited and formatted. The final version may differ from this version.



## Abstract

We investigated the intrinsic transport activity of mouse and monkey Mrp2 and compared it with that of rat and dog Mrp2 reported previously. Mrp2 cDNAs were isolated from BALB/c and Macaca fascicularis liver, respectively, and vesicle transport studies were performed using recombinant Mrp2s expressed in insect Sf9 cells. ATP-dependent transport of [$^3$H]$LTC_4$, [$^3$H]$E_2$17ßG, [$^3$H]BSP, and [$^3$H]CCK-8 were readily detected for all Mrp2s. A species difference in the intrinsic transport activity was apparent for $LTC_4$ (monkey > mouse, dog > rat) and BSP (rat, dog, monkey > mouse). In addition to the difference in the transport activity, complex kinetic profiles were also evident in CCK-8, where a cooperative transport site was observed. Moreover, the transport of [$^3$H]$E_2$17ßG by mouse and monkey Mrp2 was quite different from rat and dog Mrp2 in that, 1) there was practically only non-saturable uptake for [$^3$H]$E_2$17ßG, 2) 4-methylumbelliferon glucuronide (Mrp2 modulator) showed a concentration-dependent stimulatory effect on the transport of [$^3$H]$E_2$17ßG in mouse and monkey Mrp2, while rat and dog transport activity was inhibited by the modulator. In conclusion, while the substrate specificity is similar, the intrinsic transport activity differs from one species to another. This is due not only to the difference in the $K_m$ and $V_{max}$ values, but also the qualitatively different mode of substrate and modulator recognition exhibited by different species.

## Introduction

The multidrug resistance-associated protein 2 / ATP-binding cassette transporter family C2 (MRP2 /ABCC2) is the second of nine members of the MRP family. It is localized at the apical (canalicular) membrane of hepatocytes and involved in the phase III biliary excretion of a wide range of organic anions, including glutathione conjugates, glucuronide conjugates, sulfated conjugates of bile salt, as well as nonconjugated compounds ((Keppler and Konig, 2000; Suzuki and Sugiyama, 2002; Hoffmann and Kroemer, 2004; Fardel et al., 2005), see also the TP-search (http://133.9.194.61/tp-search/)). Extrahepatic expression was also found on the brush border membrane of the small intestine (Mottino et al., 2000; Van Aubel et al., 2000), renal epithelia of the proximal tubules (Schaub et al., 1997; Schaub et al., 1999), the luminal membrane of endothelial cells of the small blood capillaries in rat brain(Miller et al., 2000), and in the apical syncytiotrophoblast membrane of the term placenta(St-Pierre et al., 2000). The in vivo function and transport properties of Mrp2 have been well characterized in rats because mutant strains lacking Mrp2, Eisai-hyperbilirubinemic rats (EHBR) (Mikami et al., 1986) and GY/TR$^-$ rats (Jansen et al., 1985; Kuipers et al., 1989) have been available for a long time. These mutant rats are also a good animal model of Dubin-Johnson syndrome. After cloning rat Mrp2(Buchler et al., 1996; Paulusma et al., 1996; Ito et al., 1997) and human (Taniguchi et al., 1996; Paulusma et al., 1997) MRP2 cDNA, characterization of Mrp2/MRP2 transport properties has also

DMD Fast Forward. Published on August 25, 2006 as DOI: 10.1124/dmd.106.010991
This article has not been copyedited and formatted. The final version may differ from this version.



been carried out (Madon et al., 1997; Evers et al., 1998; Ito et al., 1998; Cui et al., 1999; Kawabe et al., 1999). Cui et al. were the first to compare the transport characteristics of human MRP2 and rat Mrp2 in a homogenous expression system in human embryonic kidney (HEK) 293 cells or Mardin Darby Canine Kidney (MDCK) cells (Cui et al., 1999). They confirmed that the transport kinetics of $LTC_4$ and $E_2$17ßG transport as well as acquired drug resistance profiles were similar in humans and rats. Recently, Mrp2 knockout mice have been established and a phenotype similar to EHBR or $TR^-$ was observed (Chu et al., 2006); i.e. exhibiting elevated serum total bilirubin and urine bilirubin glucuronide, with a reduced biliary excretion rate of GSH and bilirubin glucuronide. Moreover, the biliary excretion rate of intravenously administered dibromosulfophthalein, a typical Mrp2 substrate, was also impaired as seen in Mrp2-deficient rats and patients with Dubin-Johnson syndrome (Chu et al., 2006). This accumulated evidence has confirmed the common physiological function of MRP2/Mrp2 in the liver of various species as a major efflux transporter of organic anions. Strictly speaking, however, the species differences in the substrate specificity and transport activity of Mrp2 protein are not yet fully understood. It has been proposed that the in vivo biliary excretion clearance of potential Mrp2 substrates differs considerably among species (Ishizuka et al., 1999). Moreover, in vitro canalicular membrane vesicle (CMV) experiments also confirmed that there was a large species difference in the ATP-dependent transport activity of

organic anions (Ishizuka et al., 1999; Niinuma et al., 1999). Moreover, it is now widely accepted that MRP2/Mrp2 has complex substrate recognition sites as demonstrated by in vitro vesicle transport as well as cellular transport experiments (Van Aubel et al., 1999; Bakos et al., 2000; Evers et al., 2000; Bodo et al., 2003; Lou et al., 2003; Zelcer et al., 2003; Gerk et al., 2004; Ito et al., 2004; Borst et al., 2006), although we do not know whether this holds true for other species or not.

In this report we have constructed, for the first time, in vitro expression systems of mouse and monkey Mrp2 to quantitatively compare the intrinsic transport functions and properties under homogeneous conditions and compare them with previously reported rat and dog Mrp2 (Ninomiya et al., 2005) ; we found a similar substrate specificity although the kinetic profiles differed from one species to another.

## Methods

**Materials.** [$^3$H]$E_2$17ßG (55 Ci/mmol, 97 %) and [$^3$H]$LTC_4$ (100 Ci/mmol, 95 %) were purchased from PerkinElmer Life Sciences (Boston, MA). [$^3$H]cholecystokinin octapeptide (CCK-8, C-terminally sulfated octapeptide cholecyctokinin-8) (68.0 Ci/mmol) and [$^3$H]BSP (5-25 Ci/mmol) were kindly provided by Prof. Y. Sugiyama, Tokyo University. Unlabeled compounds were purchased as follows: $E_2$17βG, BSP, and 4-methylumbelliferyl-ß-D-glucuronide (4-MUG) from Sigma (St Louis, MO), $LTC_4$ from Cayman Chemical (Ann Arbor, MI), CCK-8 from Peptide Institute, Inc (Osaka, Japan). All other chemicals were of analytical grade. Sf9 cells were maintained as a suspension culture at 27 ºC with serum-free EX-CELL™ 420 medium (JRH Biosciences, Inc. Lenexa, KS). The Macaca fascicularis liver was kindly donated by Sankyo Co., Ltd. (Tokyo, Japan).

**Plasmid construction.** To obtain mouse Mrp2 cDNA, polymerase chain reaction (PCR) was performed using the forward primer [5'-aaacccAGCGCTgccatggacgaattctgcaactctacttttgg-3', which includes the *Aor*51HI site (single underline)] and the reverse primer [5'-cagggaAAGCTTctagagctccgtgtggttcacactttcaatgcc-3', which includes the *Hin*dIII site (double underline)] with BALB/c mouse liver cDNA by KOD-plus DNA polymerase (Toyobo Co., Ltd Osaka, Japan). Similarly, monkey Mrp2 cDNA was amplified using the forward primer [5'-cgcagtAGCGCTgccatgccggaggacttctgcaactctacttttgg-3', which includes the

*Aor*51HI site (single underline)] and the reverse primer [5'-gggtttAAGCTTcaaagaatgctgttcacattctcaatgcc-3', which includes the *Hin*dIII site (double underline)] from monkey liver. Reactions took place at 94°C for 2 min, followed by 30 cycles of 94°C for 15 sec, 55°C for 10 sec and 68°C for 5 min. PCR products of approximately 4.6-kilobases were subsequently digested at the *Hin*dIII site located in the reverse primer sequence. This fragment was inserted into pBluescript II SK(-) (Stratagene, LA Jolla,CA) digested with *Sma*I - *Hin*dIII in the multiple cloning site of the vector and its sequence was analyzed. To construct the baculovirus expression vector, the Mrp2 cDNA cassette was digested with *Aor*51HI and *Hin*dIII and inserted into the *Sma*I-*Hin*dIII site of recombinant donor plasmid after removing the rat Mrp2 cDNA cassette from the previously reported rat Mrp2-pFASTBAC1 using the same enzyme combination (Ito et al., 2001). Homologous recombination in *E. coli* DH10BAC was performed according to the manufacturer's instructions to obtain the recombinant bacmid and subsequent recombinant baculoviruses in Sf9 cells (Ninomiya et al., 2005). Preparation of membrane vesicles from Sf9 cells infected with recombinant Mrp2 baculoviruses was carried out as reported previously (Ninomiya et al., 2005).

**Production of standard antigen for mouse and monkey Mrp2.** The cDNA fragments encoding the carboxy terminal 53 amino acids of mouse and monkey Mrp2 were amplified from cDNA of mouse and monkey liver using the universal forward primer [5'-cacaggGAATTCaccatcatggacagtgac-3' with

*Eco*RI linker (underline)] and respective reverse primer [5'-ggaaccGTCGACtagagctccgtgtggttc-3' for mouse, 5'-tttggaGTCGACtcaaagaatgctgttcac-3' for monkey with the *Sal*I site (double underlines)]. PCR products of approximately 170 bases were subsequently digested with *Eco*RI-*Sal*I then inserted into the *Eco*RI-*Sal*I site of pMAL™-c2 vector (New England Biolabs, Inc., Beverly, MA). These vectors were transformed into *E. coli*-competent DH5α to produce standard antigens fused with maltose binding protein (MBP). After induction with 0.3 mM isopropyl-β-D-galactopyranoside for 2 h at 37 ºC, total *E. coli* lysates were subjected to SDS-polyacrylamine gel electrophoresis (PAGE) followed by Coomassie Brilliant Blue staining to quantify the amount of protein by densitometry analysis in comparison with bovine serum albumin (BSA) as a standard.

**Western blot analysis.** Samples were loaded onto an SDS-PAGE (8.5 %) and then transferred to an Immobilon™-P Transfer Membrane filter (Millipore Corp., Bedford, MA) by electroblotting. The filter was blocked at room temperature for 1 h with Tris-buffered saline with 0.05 % Tween 20 (TTBS) containing 3 % BSA and probed at room temperature for 1 h with primary antisera diluted with TTBS containing 0.1 % BSA. The antisera used were rabbit anti-rat Mrp2 antiserum and anti-human MRP2 antiserum raised against the carboxy terminal amino acid residues of 1530-1541 for rats (Buchler et al., 1996) and 1534-1545 for humans (Schaub et al., 1999),

respectively. The filters were incubated at room temperature for 1 h with donkey anti-rabbit IgG conjugated with horseradish peroxidase (Santa Cruz Biotechnology, Santa Cruz, CA) diluted with TTBS containing 0.1 % BSA (1:3000) and examined using the enhanced chemiluminescence detection kit (Amersham Biosciences, Piscataway, NJ). Images were analyzed using an LAS1000 chemiluminescence detector (Fuji photo film Co. Ltd., Tokyo, Japan). The Mrp2 expression level was calculated from the band density using mouse and monkey Mrp2 carboxy terminal antigens fused with MBP as standards. The serial dilution and the exposure time were chosen so that the densities were in the linear range.

**Transport study.** The vesicle transport study was performed using the rapid filtration technique described previously (Ninomiya et al., 2005). Briefly, 16 µl transport medium (10 mM Tris, 250 mM sucrose, 10 mM $MgCl_2$, 5 mM ATP or AMP, pH 7.4) containing radiolabeled compounds (5 nM [$^3$H]$LTC_4$, 50 nM [$^3$H]$E_2$17βG, 70 nM [$^3$H]BSP, 3 nM [$^3$H]CCK-8) was preincubated for 3 min at 25 ºC ($LTC_4$) or 37 ºC ($E_2$17βG, BSP, CCK-8) and then rapidly mixed with 4 µl membrane vesicle suspension (2-5 µg protein). The transport reaction was stopped by the addition of 1 ml ice-cold buffer (250 mM sucrose, 100 mM NaCl, 10 mM Tris-HCl, pH 7.4). The stopped reaction mixture was passed through a 0.45-µm HAWP filter (Millipore Corp.) and then washed twice with 5 ml stop buffer. The radioactivity retained on the filter was determined using a liquid scintillation counter (LSC5000, Aloka Co.,

Tokyo, Japan). ATP-dependent transport was calculated by subtracting the transport in the presence of AMP from that in the presence of ATP. In some cases, the Mrp2-dependent transport was calculated by subtracting the transport into green fluorescent protein (GFP)-expressing vesicles (GFP-control) from that into Mrp2-expressing vesicles in the presence of ATP as described previously (Ito et al., 2001; Ninomiya et al., 2005). The intrinsic transport activities of Mrp2 were obtained by dividing the Mrp2-dependent transport of these ligands (pmol/min/mg protein) by the absolute Mrp2 expression level (nmol Mrp2/mg protein). Kinetic parameters for the transport of [$^3$H]$LTC_4$ (rat, dog) and CCK-8 (mouse and monkey) were estimated from the following equation(Ninomiya et al., 2005):

$$v = V_{max} \times S^n/(K_m + S^n)$$

where v is the transport rate, $V_{max}$ is the maximum transport rate, S is the ligand concentration, n is the Hill coefficient, and $K_m$ is the Michaelis constant. Kinetic parameters for the transport of [$^3$H]$E_2$17βG were estimated from the following equation :

$$v = V_{max} \times S/(K_m + S) + PS_{ns} \times S$$

where $PS_{ns}$ is the non-saturable component (μl/min/mg protein). The conventional Michaelis-Menten equation (without the Hill coefficient and non-saturable component) was used for the other cases. The kinetic data were fitted to the above equations by an iterative nonlinear least-squares method using the MULTI program to obtain kinetic parameters (Yamaoka et al., 1981).

The input data were weighted as the reciprocal of the square of the observed values, and the Damping Gauss-Newton algorithm was used for fitting.

## Results

**Isolation of Mouse and Monkey Mrp2.** Cloned mouse (BALB/c) and monkey (Macaca fascicularis) Mrp2 cDNA consisted of 4,629 bp and 4,632 bp open reading frames encoding the 1543 and 1544 predicted amino acid sequences, respectively. They contained 19 and 21 nucleotide substitutions which led to 11 amino acid mutations compared with the reported mouse and monkey Mrp2 sequences (Genbank accession of AF282772 (AKR/J), AF282773 (C57L/J), AF227274 and NM_013806 (house mouse) and AF410948, NM_001032847 and DQ015923 (Macaca mulatta)) (Fig.1). These nucleotide substitutions were also identified by direct sequencing analysis of the PCR product amplified from the livers (data not shown). We therefore considered substitutions as genetic polymorphisms and the cDNA products were further processed for recombinant protein expression in insect Sf9 cells.

**Quantification of mouse and monkey Mrp2 protein expression in the membrane vesicles.** We tried to detect mouse and monkey Mrp2 protein in a quantitative manner using two kinds of antisera produced originally following immunization against rat and human c-terminal-directed Mrp2/MRP2 as described previously (Ninomiya et al., 2005). Anti-rat Mrp2 and anti-human MRP2 antisera successfully detected mouse and monkey Mrp2 standard peptides (c-terminal 53 amino acids) fused with MBP at a molecular weight of 48 kD, respectively (Fig. 2). Recombinant mouse and monkey

Mrp2 proteins were also detected at a molecular weight of 175 kD with these antisera (Fig. 2). Using these antisera, mouse and monkey Mrp2 protein was quantified in comparison with the standard peptides. The calculated expressions were 261 ± 41 pmol Mrp2/mg protein and 311 ± 104 pmol Mrp2/mg protein for mouse and monkey Mrp2, respectively. These expression levels are in the same range as the rat and dog Mrp2 expression level in the same experimental system reported previously (524 ± 55 and 409 ± 21 pmol Mrp2/mg protein for rat and dog Mrp2, respectively (Ninomiya et al., 2005)).

**Transport of typical Mrp2 substrates.** Clear time- and ATP-dependent transport was observed using typical Mrp2 substrates, $LTC_4$ (glutathione conjugate), $E_2$17ßG (glucuronide conjugate), BSP (unconjugated anion), and CCK-8 (C-terminally sulfated octapeptide). ATP-dependent transport was negligible in GFP-control vesicles and transport in the presence of AMP did not differ significantly from one type of vesicle to another (data not shown). The initial rates of ATP-dependent transport ($LTC_4$, 30 sec at 25°C; $E_2$17ßG, 30 sec at 37°C; BSP, 3 min at 37°C; CCK-8, 3 min at 37°C) were normalized by the absolute Mrp2 protein expression (Table 1). As a result, intrinsic transport activity was not the same among species. In the case of $LTC_4$, the transport activity of monkey Mrp2 was more than 10 times higher than that of rat Mrp2 (33.7 pmol/min/nmol Mrp2 (monkey) vs. 2.57 pmol/min/nmol Mrp2 (rat)) (Table 1). Moreover, the rank order of intrinsic

transport activity was not the same among substrates; $LTC_4$ [monkey > mouse > dog > rat (ranging from 2.57 to 33.7 pmol/min/nmol Mrp2)], BSP [rat, dog, monkey > mouse (ranging from 9.51 to 45.7 pmol/min/nmol Mrp2)]. Similar intrinsic transport activities were observed for $E_2$17ßG (ranging from 3.57 to 8.33 pmol/min/pmol Mrp2) and CCK-8 (ranging from 0.77 to 1.35 pmol/min/pmol Mrp2).

**Concentration-dependence of the substrate transport.** The initial rates of the Mrp2-dependent transport were determined for a range of substrate concentrations : $LTC_4$ (0.05-35 µM), $E_2$17ßG (0.1-600 µM dissolved finally in 0.2 % DMSO), BSP (0.07–50 µM), and CCK-8 (0.07–32 µM). $LTC_4$ transport in mouse and monkey Mrp2 was fitted to a normal Michaelis-Menten equation, although rat and dog Mrp2 exhibited a homotropic cooperativity curve with a Hill coefficient of 1.16 ± 0.22 and 1.30 ± 0.04, respectively(Ninomiya et al., 2005). The rank order of the $K_m$ values of [$^3$H]$LTC_4$ was dog (0.53 µM) < mouse and monkey (0.65 µM) < rat (2.05 µM) (Table 1), while that of the $V'_{max}$ values ($V_{max}$ normalized by Mrp2 expression) was dog (2.88 pmol/min/pmol Mrp2), rat (2.97 pmol/min/pmol Mrp2) < mouse (3.92 pmol/min/pmol Mrp2) < monkey (6.56 pmol/min/pmol Mrp2). There was a marked species difference in the concentration-dependent profile of [$^3$H]$E_2$17βG transport (Fig.4 and supplement 1). The ATP-dependent transport was virtually unsaturated in mouse and monkey even in the presence of 600 µM $E_2$17ßG. This was actual transport into the vesicles, not mere

DMD Fast Forward. Published on August 25, 2006 as DOI: 10.1124/dmd.106.010991
This article has not been copyedited and formatted. The final version may differ from this version.



surface binding, because clear osmotic sensitivity was confirmed (data not shown). Although comparable $K_m$ (2.96 ~ 5.35 μM) and $V'_{max}$ (3.70 ~ 7.98 pmol/min/pmol mrp2) values were obtained for the transport of BSP, both $K_m$ and $V'_{max}$ contribute to the lowest intrinsic transport activity in mouse Mrp2; mouse Mrp2 has the highest $K_m$ (5.35 μM) and lowest $V'_{max}$ (3.70 pmol/min/pmol Mrp2). The concentration-dependence of CCK-8 transport was qualitatively different among the species (Fig. 4 and supplement 1). Rat and dog Mrp2 followed a simple Michaelis-Menten equation, while mouse and monkey Mrp2 exhibited typical allosteric behavior with a Hill coefficient of 1.86 ± 0.17 and 1.18 ± 0.14, respectively (Fig. 4, Table 1 and supplement 1).

**Effect of transport modulators on the transport of [$^3$H]$E_2$17ßG**. To further characterize the mode of interaction between Mrp2 and glucuronide conjugates, we examined the effect of another glucuronide conjugate, 4-MUG, a glucuronide conjugate form of 4-MU, on the transport of [$^3$H]$E_2$17ßG (25 nM). Notably, 4-MUG never inhibited but actually stimulated the transport by mouse and monkey Mrp2 in a concentration-dependent manner (Fig. 5), while that of rat and dog Mrp2 only had an inhibitory effect (Ninomiya et al., 2005). MRP2/Mrp2 transport activity is modulated (inhibited or stimulated) by a series of compounds implying the presence of multiple recognition sites for substrate and modulator. To obtain insight into the species difference in the recognition system of the substrate and modulator, $E_2$17βG transport activity was measured in the presence of known modulators, indomethacin (IM) and

taurocholate (TC). As shown in Fig. 6, both compounds stimulated all Mrp2s, suggesting the presence of a conserved binding site at least for these two modulators.

DMD Fast Forward. Published on August 25, 2006 as DOI: 10.1124/dmd.106.010991
This article has not been copyedited and formatted. The final version may differ from this version.



**Discussion**

All Mrp2s accepted typical Mrp2 substrates, indicating similar substrate specificity (Fig. 3). Except for $E_2$17ßG, the overall transport affinities ($K_m$) were comparable among these species ($LTC_4$; 0.53~2.05 µM, BSP; 2.96~5.35 µM, CCK-8; 2.37~9.79 µM). These were also similar to human MRP2 determined in a recombinant vesicle study (1.0 µM for $LTC_4$, 8,1 µM for CCK-8 (Letschert et al., 2005)). Strictly speaking, however, a marked difference in the intrinsic transport activity (normalized by the protein expression in the vesicles) was observed among the species (Table 1). This is due not only to the differences in $K_m$ and $V_{max}$ values, but also to the presence of a cooperative transport site for some compounds (Table 1). The most striking difference in the transport kinetics involves $E_2$17ßG. Homotropic cooperativity of $E_2$17βG transport by MRP2/Mrp2 has been reported independently by several groups (Bodo et al., 2003; Zelcer et al., 2003; Gerk et al., 2004). These authors found that a plot of initial transport rate versus concentration shows an S-curve, rather than the standard hyperbolic substrate saturation curve. However, we did not see any cooperative effect for $E_2$17ßG transport in all animal Mrp2s tested. Alternatively, an additional multiple, but independent, low affinity transport site was observed in rat and dog Mrp2, which was not saturated up to 600 µM (Fig. 4 and (Ninomiya et al., 2005)) and only a non-saturable site was found in mouse and monkey Mrp2. Supporting the qualitative difference between rat/dog Mrp2s and mouse/monkey Mrp2s

DMD Fast Forward. Published on August 25, 2006 as DOI: 10.1124/dmd.106.010991
This article has not been copyedited and formatted. The final version may differ from this version.



related to the $E_2$17ßG transport, the former Mrp2s were inhibited while the latter Mrp2s were stimulated by 4-MUG (present study and (Ninomiya et al., 2005)). Mrp2 seems to have multiple recognition sites for glucuronide conjugates, although it depends on the Mrp2 species whether they have an inhibitory (rat and dog) or stimulatory (mouse and monkey) effect. It is presently unknown why such a discrepancy exists between the reported homotropic cooperativity of $E_2$17ßG transport by rat Mrp2 (Gerk et al., 2004) and our data showing no cooperativity. One possible reason is the difference in the Mrp2 expression level between different laboratories. In our case, ATP-dependent transport of $E_2$17ßG was as high as 5.5 pmol/mg protein at 1 min (50 nM), while other authors obtained a value of 1.5 pmol/mg protein at 1 min (77 nM) (Gerk et al., 2004). The calculated uptake clearance (uptake velocity divided by substrate concentration) was 5.6-fold higher in our rat Mrp2 expression system. Moreover, the initial uptake velocity was determined at different time points : 0-30 second uptake in our system but 2-5 minute uptake in another study(Gerk et al., 2004). The effect of these different experimental conditions on the transport kinetics remains to be determined.

Heterotropic cooperative transport sites have been widely known for MRP2 as well as other MRP family members. Loe et al initially found that vincristine (VCR) transport by MRP1 is stimulated by GSH. Reciprocally, VCR stimulates GSH transport and reduces the Km for GSH from >1mM to 100 μM(Loe et al., 1998). Since then, such stimulated transport has been

further demonstrated in other MRP family members using a vesicular transport system as well as in intact cells (Van Aubel et al., 1999; Bakos et al., 2000; Evers et al., 2000; Huisman et al., 2002; Bodo et al., 2003; Lou et al., 2003; Zelcer et al., 2003; Gerk et al., 2004; Ito et al., 2004; Huisman et al., 2005). Bakos et al. demonstrated a difference in the modulation profile of N-ethylmaleimide glutathione (NEM-GS) transport by human MRP1 and MRP2 expressed in Sf9 cells. NEM-GS transport by MRP2 was stimulated by penicillin G, sulfynpyrazone, and IM, while MRP1 was stimulated by IM but inhibited by sulfynpyrazone (Bakos et al., 2000). $E_2$17ßG transport by MRP2 was stimulated by IM (600-1200 % in the presence of 100μM IM), while MRP3 was slightly stimulated only at a low concentration and inhibited at a higher concentration (>50 μM) (Bodo et al., 2003). This accumulating evidence indicates that the MRP family has similar but distinct modulator sensitivities. As for animal Mrp2s, IM similarly stimulated the transport of $E_2$17ßG but this stimulatory effect was saturated or even reduced at concentrations higher than 100 μM (Fig. 6). The inhibitory effect at higher concentrations is explained by the model proposed by Borst et al. (Borst et al., 2006). In this model, the modulator (M) binds to an allosteric site (M site) and this binding increases the affinity of the transport site (S site) for the substrate (S) (heterotropic cooperativity or stimulated transport). M may not be transported at all, but if S can also bind to the M-site, it may stimulate its own transport (homotropic cooperativity). Applying our results to this model,

$LTC_4$ can not only bind to the S site but also to the M site of rat and dog Mrp2. The same is true for CCK-8, where it binds not only to the S site but also to the M site of mouse and monkey Mrp2. Alternatively, the affinity of $LTC_4$ and CCK-8 for the M site is too high to be detected (almost saturated at a tracer concentration) in Mrp2 species lacking homotropic cooperativity. Interestingly, the absolute transport activities (normalized by Mrp2 protein expression) approached each other in the presence of these modulators (Fig. 6). This implies that the transport potential ($V'_{max}$ normalized by Mrp2 expression) is similar among these Mrp2 species and can be fully activated by the modulators. Supporting this consideration, Zelcer et al. reported that the maximum rate ($V_{max}$) of $E_2$17ßG transport by human MRP2 remained relatively unchanged while the affinity was increased in the presence of 100 μM IM (Zelcer et al., 2003).

Physiological significance of the heterotropic effects has not been established. De Waart et al. demonstrated that thromboxane B2 and isoprostane F2α stimulate the dinitrophenyl glutahione transport by human MRP2 expressed in Sf21 insect cells, whereas addition of physiological concentration of GSH (3 mM) abolished this effect (de Waart et al., 2006). The authors discussed that if the heterotropic effects observed for a series of modulators are all eliminated by GSH, these effects may be irrelevant in the in vivo situation as GSH concentration in the hepatocyte is high enough. In our

case, however, stimulatory effect of 4-MUG, IM and TC on the transport of $E_2$17ßG was not abolished at all in the presence of 5 mM GSH (supplement 2), implying the plurality of modulator binding sites and still room for argument about physiological significance of the heterotropic effects in vivo.

Recently, Shilling et al. compared the transport properties of $LTC_4$ and $E_2$17ßG in CMVs from rat, dog, monkey and human liver (Shilling et al., 2005). The transport characteristics were different from our present observations in that, 1) the $K_m$ values for $E_2$17ßG were higher (465 µM and 382 µM for rat and dog, respectively) compared with our results (1.39 µM and 2.13 µM for rat and dog Mrp2, respectively (Table 1) and 2) transport was saturable with a $K_m$ of 81.3 µM for the transport of $E_2$17ßG into CMV from dog, while there was no saturation in the presence of up to 600 µM $E_2$17ßG in our case. One possible reason for this discrepancy is the different concentration range of unlabeled $E_2$17ßG used in those studies (Shilling et al., 2005). We used 0.1 µM $E_2$17ßG as the lowest concentration, while they used 25 µM. Using such a high concentration range, the high affinity site might be already saturated or masked. The $K_m$ values for $E_2$17ßG reported by Shilling et al. possibly correspond to the low affinity transport sites which we were unable to cover in the present study. Another possibility is the contribution of other ABC transporters such as breast cancer resistance protein (Bcrp/Abcg2) and P-glycoprotein (Pgp/Mdr1/Abcb1) possibly expressed in dog CMV and can transport $E_2$17ßG (Huang et al., 1998; Suzuki et al., 2003).

In conclusion, although the substrate specificity is similar among Mrp2s from rat, mouse, dog and monkey, the intrinsic transport activity for respective compounds differs from one species to another even when compared in a homogenous in vitro expression system. This is due not only to the difference in the $K_m$ and $V_{max}$ values, but also to the qualitatively different substrate and modulator recognition sites found in the different species.

## References

Bakos E, Evers R, Sinko E, Varadi A, Borst P and Sarkadi B (2000) Interactions of the human multidrug resistance proteins MRP1 and MRP2 with organic anions. *Mol Pharmacol* **57:**760-768.

Bodo A, Bakos E, Szeri F, Varadi A and Sarkadi B (2003) Differential modulation of the human liver conjugate transporters MRP2 and MRP3 by bile acids and organic anions. *J Biol Chem* **278:**23529-23537.

Borst P, Zelcer N, van de Wetering K and Poolman B (2006) On the putative co-transport of drugs by multidrug resistance proteins. *FEBS Lett* **580:**1085-1093.

Buchler M, Konig J, Brom M, Kartenbeck J, Spring H, Horie T and Keppler D (1996) cDNA cloning of the hepatocyte canalicular isoform of the multidrug resistance protein, cMrp, reveals a novel conjugate export pump deficient in hyperbilirubinemic mutant rats. *J Biol Chem* **271:**15091-15098.

Chu X, Strauss JR, Mariano MA, Li J, Newton DJ, Cai X, Wang RW, Yabut J, Hartley DP, Evans DC and Evers R (2006) Characterization of Mice Lacking the Multidrug Resistance Protein Mrp2 (Abcc2). *J Pharmacol Exp Ther*.

Cui Y, Konig J, Buchholz JK, Spring H, Leier I and Keppler D (1999) Drug resistance and ATP-dependent conjugate transport mediated by the apical multidrug resistance protein, MRP2, permanently expressed in human and canine cells. *Mol Pharmacol* **55:**929-937.

de Waart DR, Paulusma CC, Kunne C and Oude Elferink RP (2006) Multidrug resistance associated protein 2 mediates transport of prostaglandin E. *Liver Int* **26:**362-368.

Evers R, de Haas M, Sparidans R, Beijnen J, Wielinga PR, Lankelma J and Borst P (2000) Vinblastine and sulfinpyrazone export by the multidrug resistance protein MRP2 is associated with glutathione export. *Br J Cancer* **83:**375-383.

Evers R, Kool M, van Deemter L, Janssen H, Calafat J, Oomen LC, Paulusma CC, Oude Elferink RP, Baas F, Schinkel AH and Borst P (1998) Drug export activity of the human canalicular multispecific organic anion transporter in polarized kidney MDCK cells expressing cMOAT (MRP2) cDNA. *J Clin Invest* **101:**1310-1319.

Fardel O, Jigorel E, Le Vee M and Payen L (2005) Physiological, pharmacological and clinical features of the multidrug resistance protein 2. *Biomed Pharmacother* **59:**104-114.

Gerk PM, Li W and Vore M (2004) Estradiol 3-glucuronide is transported by the multidrug resistance-associated protein 2 but does not activate the allosteric site bound by estradiol 17-glucuronide. *Drug Metab Dispos* **32:**1139-1145.

Hoffmann U and Kroemer HK (2004) The ABC transporters MDR1 and MRP2: multiple functions in disposition of xenobiotics and drug resistance. *Drug Metab Rev* **36:**669-701.

Huang L, Hoffman T and Vore M (1998) Adenosine triphosphate-dependent transport of estradiol-17beta(beta-D-glucuronide) in membrane vesicles by MDR1 expressed in insect cells. *Hepatology* **28:**1371-1377.

Huisman MT, Chhatta AA, van Tellingen O, Beijnen JH and Schinkel AH (2005) MRP2 (ABCC2) transports taxanes and confers paclitaxel resistance and both processes are stimulated by probenecid. *Int J Cancer* **116:**824-829.

Huisman MT, Smit JW, Crommentuyn KM, Zelcer N, Wiltshire HR, Beijnen JH and Schinkel AH (2002) Multidrug resistance protein 2 (MRP2) transports HIV protease inhibitors, and transport can be enhanced by other drugs. *Aids* **16:**2295-2301.

Ishizuka H, Konno K, Shiina T, Naganuma H, Nishimura K, Ito K, Suzuki H and Sugiyama Y (1999) Species differences in the transport activity for organic anions across the bile canalicular membrane. *J Pharmacol Exp Ther* **290:**1324-1330.

Ito K, Koresawa T, Nakano K and Horie T (2004) Mrp2 is involved in benzylpenicillin-induced choleresis. *Am J Physiol Gastrointest Liver Physiol* **287:**G42-49.

Ito K, Suzuki H, Hirohashi T, Kume K, Shimizu T and Sugiyama Y (1997) Molecular cloning of canalicular multispecific organic anion transporter defective in EHBR. *Am J Physiol* **272:**G16-22.

Ito K, Suzuki H, Hirohashi T, Kume K, Shimizu T and Sugiyama Y (1998) Functional analysis of a canalicular multispecific organic anion transporter cloned from rat liver. *J Biol Chem* **273:**1684-1688.

Ito K, Suzuki H and Sugiyama Y (2001) Charged amino acids in the transmembrane domains are involved in the determination of the substrate specificity of rat Mrp2. *Mol Pharmacol* **59:**1077-1085.

Jansen PL, Peters WH and Lamers WH (1985) Hereditary chronic conjugated hyperbilirubinemia in mutant rats caused by defective hepatic anion transport. *Hepatology* **5:**573-579.

Kawabe T, Chen ZS, Wada M, Uchiumi T, Ono M, Akiyama S and Kuwano M (1999) Enhanced transport of anticancer agents and leukotriene C4 by the human canalicular multispecific organic anion transporter (cMOAT/MRP2). *FEBS Lett* **456:**327-331.

Keppler D and Konig J (2000) Hepatic secretion of conjugated drugs and endogenous substances. *Semin Liver Dis* **20:**265-272.

Kuipers F, Radominska A, Zimniak P, Little JM, Havinga R, Vonk RJ and Lester R (1989) Defective biliary secretion of bile acid 3-O-glucuronides in rats with hereditary conjugated hyperbilirubinemia. *J Lipid Res* **30:**1835-1845.

Letschert K, Komatsu M, Hummel-Eisenbeiss J and Keppler D (2005) Vectorial transport of the peptide CCK-8 by double-transfected MDCKII cells stably expressing the organic anion transporter OATP1B3 (OATP8) and the export pump ABCC2. *J Pharmacol Exp Ther* **313:**549-556.

Loe DW, Deeley RG and Cole SP (1998) Characterization of vincristine transport by the M(r) 190,000 multidrug resistance protein (MRP): evidence for cotransport with reduced glutathione. *Cancer Res* **58:**5130-5136.

Lou H, Ookhtens M, Stolz A and Kaplowitz N (2003) Chelerythrine stimulates GSH transport by rat Mrp2 (Abcc2) expressed in canine kidney cells. *Am J Physiol Gastrointest Liver Physiol* **285:**G1335-1344.

Madon J, Eckhardt U, Gerloff T, Stieger B and Meier PJ (1997) Functional expression of the rat liver canalicular isoform of the multidrug resistance-associated protein. *FEBS Lett* **406:**75-78.

Mikami T, Nozaki T, Tagaya O, Hosokawa S, Nakura T, Hori H and Kondou S (1986) The characters of a new mutant rats with hyperbilirubinuria syndrome. *Cong Anom* **26:**250-251.

Miller DS, Nobmann SN, Gutmann H, Toeroek M, Drewe J and Fricker G (2000) Xenobiotic transport across isolated brain microvessels studied by confocal microscopy. *Mol Pharmacol* **58:**1357-1367.

Mottino AD, Hoffman T, Jennes L and Vore M (2000) Expression and localization of multidrug resistant protein mrp2 in rat small intestine. *J Pharmacol Exp Ther* **293:**717-723.

Niinuma K, Kato Y, Suzuki H, Tyson CA, Weizer V, Dabbs JE, Froehlich R, Green CE and Sugiyama Y (1999) Primary active transport of organic anions on bile canalicular membrane in humans. *Am J Physiol* **276:**G1153-1164.

Ninomiya M, Ito K and Horie T (2005) Functional analysis of dog multidrug resistance-associated protein 2 (Mrp2) in comparison with rat Mrp2. *Drug Metab Dispos* **33:**225-232. Epub 2004 Oct 2026.

Paulusma CC, Bosma PJ, Zaman GJ, Bakker CT, Otter M, Scheffer GL, Scheper RJ, Borst P and Oude Elferink RP (1996) Congenital jaundice in rats with a mutation in a multidrug resistance- associated protein gene. *Science* **271:**1126-1128.

Paulusma CC, Kool M, Bosma PJ, Scheffer GL, ter Borg F, Scheper RJ, Tytgat GN, Borst P, Baas F and Oude Elferink RP (1997) A mutation in the human canalicular multispecific organic anion transporter gene causes the Dubin-Johnson syndrome. *Hepatology* **25:**1539-1542.

Schaub TP, Kartenbeck J, Konig J, Spring H, Dorsam J, Staehler G, Storkel S, Thon WF and Keppler D (1999) Expression of the MRP2 gene-encoded conjugate export pump in human kidney proximal tubules and in renal cell carcinoma. *J Am Soc Nephrol* **10:**1159-1169.

Schaub TP, Kartenbeck J, Konig J, Vogel O, Witzgall R, Kriz W and Keppler D

(1997) Expression of the conjugate export pump encoded by the mrp2 gene in the apical membrane of kidney proximal tubules. *J Am Soc Nephrol* **8:**1213-1221.

Shilling AD, Azam F, Kao J and Leung L (2005) Use of canalicular membrane vesicles (CMVs) from rats, dogs, monkeys and humans to assess drug transport across the canalicular membrane. *J Pharmacol Toxicol Methods*.

St-Pierre MV, Serrano MA, Macias RI, Dubs U, Hoechli M, Lauper U, Meier PJ and Marin JJ (2000) Expression of members of the multidrug resistance protein family in human term placenta. *Am J Physiol Regul Integr Comp Physiol* **279:**R1495-1503.

Suzuki H and Sugiyama Y (2002) Single nucleotide polymorphisms in multidrug resistance associated protein 2 (MRP2/ABCC2): its impact on drug disposition. *Adv Drug Deliv Rev* **54:**1311-1331.

Suzuki M, Suzuki H, Sugimoto Y and Sugiyama Y (2003) ABCG2 transports sulfated conjugates of steroids and xenobiotics. *J Biol Chem* **278:**22644-22649.

Taniguchi K, Wada M, Kohno K, Nakamura T, Kawabe T, Kawakami M, Kagotani K, Okumura K, Akiyama S and Kuwano M (1996) A human canalicular multispecific organic anion transporter (cMOAT) gene is overexpressed in cisplatin-resistant human cancer cell lines with decreased drug accumulation. *Cancer Res* **56:**4124-4129.

Van Aubel RA, Hartog A, Bindels RJ, Van Os CH and Russel FG (2000) Expression and immunolocalization of multidrug resistance protein 2 in rabbit small intestine. *Eur J Pharmacol* **400:**195-198.

Van Aubel RA, Koenderink JB, Peters JG, Van Os CH and Russel FG (1999) Mechanisms and interaction of vinblastine and reduced glutathione transport in membrane vesicles by the rabbit multidrug resistance protein Mrp2 expressed in insect cells. *Mol Pharmacol* **56:**714-719.

Yamaoka K, Tanigawara Y, Nakagawa T and Uno T (1981) A pharmacokinetic analysis program (multi) for microcomputer. *J Pharmacobiodyn* **4:**879-885.

Zelcer N, Huisman MT, Reid G, Wielinga P, Breedveld P, Kuil A, Knipscheer P, Schellens JH, Schinkel AH and Borst P (2003) Evidence for two interacting ligand binding sites in human multidrug resistance protein 2 (ATP binding cassette C2). *J Biol Chem* **278:**23538-23544.

**Footnote**

This work was supported in part by a Grant-in-Aid for Scientific Research (15790085) from the Japan Society for the Promotion of Science.

**Legends for Figures**

Figure 1. Comparison of the Mrp2 sequences (BALB/c and Macaca fascicularis) used in this study with those previously reported. Upper panels show schematic diagrams of the distribution of amino acid substitutions in mouse and monkey Mrp2s. Dots represent the approximate location of amino acid substitutions compared with the reported mouse and monkey sequences (Genbank accession No. AF282772 (AKR/J), AF282773 (C57L/J), AF282774, NM_013806 (house mouse) and DQ015923, AF410948, NM_001032847 (Macaca mulatta)). NBD, nucleotide binding domain. Alignment of the amino acids not identical among the clones extracted in the lower panels.

Figure 2. Mrp2 expression in membrane vesicles. The membrane vesicles and respective standard Mrp2 protein fused with MBP were separated on SDS-PAGE. The fractionated proteins were transferred to a membrane filter by electroblotting. Mouse Mrp2 was detected with anti-rat Mrp2 antiserum. Monkey Mrp2 was detected with anti-human MRP2 antiserum. The absolute expression of mouse and monkey Mrp2 was calculated from the standard curve of each standard Mrp2 protein. The band densities of Mrp2s in Sf9 cells were within the linear range of the respective standard Mrp2 proteins.

Figure 3. The ATP-dependent transport of typical Mrp2 substrates by Mrp2. The membrane vesicles (5-20 μg of protein) from respective rat Mrp2 (●),

mouse Mrp2 (■), dog Mrp2 (■), monkey Mrp2 (▲) and GFP (×) expressing Sf9 cells were incubated in medium containing [$^3$H]$LTC_4$ (5 nM) at 25 ºC, [$^3$H]$E_2$17ßG (50 nM) at 37 ºC, [$^3$H]BSP (70 nM) at 37 ºC, [$^3$H]CCK-8 (3 nM) at 37 ºC in the presence of 5mM ATP or AMP. Results are shown as the ATP-dependent transport calculated by subtracting the transport in the presence of AMP from that in the presence of ATP. Each point and vertical bar represent the mean ± S.D. of triplicate determinations. The data for rat and dog Mrp2 were taken from our previous report(Ninomiya et al., 2005).

Figure 4. Concentration-dependence of the transport. The transport of [$^3$H]$LTC_4$ (30 sec, at 25 ºC), [$^3$H]$E_2$17ßG (30 sec, at 37 ºC), [$^3$H]BSP (3 min, at 37 ºC), and [$^3$H]CCK-8 (3 min, at 37 ºC) was examined in the presence of various concentrations of substrates of rat Mrp2 (●), mouse Mrp2 (■), dog Mrp2 (■) and monkey Mrp2 (▲). Each symbol represents the Mrp2-dependent transport determined by subtracting the transport into GFP-control vesicles from that into Mrp2-expressing vesicles in the presence of ATP. Each point and vertical/horizontal bar represent the mean ± S.D. of triplicate determinations. Data were fitted to respective Michaelis-Menten equations as described in Materials and Methods. The data from the rat and dog Mrp2 transport experiments for $LTC_4$ and $E_2$17ßG were taken from our previous report(Ninomiya et al., 2005).

Figure 5. Effect of 4-MUG on [$^3$H]$E_2$17βG transport. The effect of 4-MUG on the transport of [$^3$H]$E_2$17βG (50 nM; for 30 sec at 37 ºC ) was examined for mouse Mrp2 (◆) and monkey Mrp2 (▲). Each symbol represents the Mrp2-dependent transport determined by subtracting the transport into GFP-expressing vesicles from that into respective Mrp2-expressing vesicles in the presence of ATP. Each point and vertical bar represent the mean ± S.D. of triplicate determinations.

Figure 6. Effect of indomethacin (IM) and taurocholate (TC) on Mrp2-mediated [$^3$H]$E_2$17βG transport activity. Transport of [$^3$H]$E_2$17βG (50 nM; for 30 sec at 37 ºC ) was examined. Rat Mrp2 (●), mouse Mrp2 (◆), dog Mrp2 (■) and monkey Mrp2 (▲). Each symbol represents the Mrp2-dependent transport determined by subtracting the transport into GFP-expressing vesicles from that into respective Mrp2-expressing vesicles in the presence of ATP. The relative transport ratio (A and B) and absolute transport rate normalized by Mrp2 expression (C and D) are shown. Each point and vertical bar represents the mean ± S.D. of triplicate determinations.

DMD Fast Forward. Published on August 25, 2006 as DOI: 10.1124/dmd.106.010991
This article has not been copyedited and formatted. The final version may differ from this version.



**Table 1.** Kinetic parameters

| $LTC_4$ | Rat* | Mouse | Dog* | Monkey |
|---|---|---|---|---|
| Transport activity (at 2.5 nM) (pmol/min/nmol Mrp2) | 2.57 ± 0.44 | 14.3 ± 0.8 | 9.76 ± 0.78 | 33.7 ± 0.1 |
| $K_m$ (μM) | 2.05 ± 0.41 | 0.65 ± 0.26 | 0.53 ± 0.03 | 0.65 ± 0.19 |
| $V_{max}$ (pmol/min/mg protein) | 1554 ± 51 | 1022 ± 86 | 1180 ± 8 | 2039 ± 168 |
| $V'_{max}$ (pmol/min/pmol Mrp2) | 2.97 ± 0.10 | 3.92 ± 0.33 | 2.88 ± 0.02 | 6.56 ± 0.54 |
| Hill coefficient | 1.16 ± 0.22 | - | 1.30 ± 0.04 | - |
| $V'_{max}/K_m$ (μL/min/pmol Mrp2) | 1.45 ± 0.29 | 6.03 ± 2.47 | 5.43 ± 0.31 | 10.1 ± 3.1 |
| **$E_2$17ßG** | **Rat** | **Mouse** | **Dog** | **Monkey** |
| Transport activity (at 25 nM) (pmol/min/nmol Mrp2) | 8.33 ± 0.86 | 3.57 ± 0.43 | 6.20 ± 0.96 | 3.58 ± 0.46 |
| $K_m$ (μM) | 1.39 ± 6.50 | - | 2.13 ± 5.67 | - |
| $V_{max}$ (pmol/min/mg protein) | 1192 ± 129 | - | 287 ± 41 | - |
| $V'_{max}$ (pmol/min/pmol Mrp2) | 2.27 ± 0.34 | - | 0.70 ± 0.11 | - |
| PS'ns (μL/min/pmol Mrp2) | 0.059 ± 0.007 | 0.064 ± 0.005 | 0.058 ± 0.002 | 0.084 ± 0.008 |
| $V'_{max}/K_m$ (μL/min/pmol Mrp2) | 1.63 ± 7.64 | - | 0.33 ± 0.88 | - |
| **BSP** | **Rat** | **Mouse** | **Dog** | **Monkey** |
| Transport activity (at 70 nM) (pmol/min/nmol Mrp2) | 45.7 ± 7.1 | 9.51 ± 3.89 | 41.8 ± 7.7 | 41.8 ± 6.1 |
| $K_m$ (μM) | 2.96 ± 0.91 | 5.35 ± 1.52 | 4.82 ± 0.47 | 4.77 ± 1.67 |
| $V_{max}$ (nmol/min/mg protein) | 2.37 ± 0.19 | 1.30 ± 0.12 | 1.77 ± 0.05 | 1.83 ± 0.20 |
| $V'_{max}$ (pmol/min/pmol Mrp2) | 6.04 ± 0.49 | 3.70 ± 0.33 | 4.90 ± 0.14 | 7.98 ± 0.86 |
| $V'_{max}/K_m$ (μL/min/pmol Mrp2) | 2.04 ± 0.65 | 0.69 ± 0.21 | 1.02 ± 0.10 | 1.67 ± 0.61 |
| **CCK-8** | **Rat** | **Mouse** | **Dog** | **Monkey** |
| Transport activity (at 3 nM) (pmol/min/nmol Mrp2) | 1.28 ± 0.16 | 0.77 ± 0.17 | 1.35 ± 0.41 | 1.30 ± 0.22 |
| $K_m$ (μM) | 3.14 ± 0.73 | 2.37 ± 0.14 | 9.79 ± 0.89 | 5.73 ± 0.90 |
| $V_{max}$ (pmol/min/mg protein) | 771 ± 41 | 469 ± 15 | 879 ± 25 | 526 ± 30 |
| $V'_{max}$ (pmol/min/pmol Mrp2) | 1.97 ± 0.11 | 1.33 ± 0.04 | 2.44 ± 0.07 | 2.29 ± 0.13 |
| Hill coefficient | - | 1.86 ± 0.17 | - | 1.18 ± 0.14 |
| $V'_{max}/K_m$ (μL/min/pmol Mrp2) | 0.63 ± 0.15 | 0.56 ± 0.04 | 0.25 ± 0.02 | 0.40 ± 0.07 |

Each value was calculated from the data shown in Fig. 3 (transport activity) and Fig. 4 (kinetic parameters). Values represent the obtained parameter ± computer calculated S.D. $V'_{max}$ and $PS'_{ns}$ values mean $V_{max}$ and $PS_{ns}$ values normalized by the absolute expression level of each Mrp2 protein, respectively.
* Cited from our previous publication (Ninomiya et al., 2005).

DMD Fast Forward. Published on August 25, 2006 as DOI: 10.1124/dmd.106.010991
This article has not been copyedited and formatted. The final version may differ from this version.

Fig. 1

## Mouse Mrp2

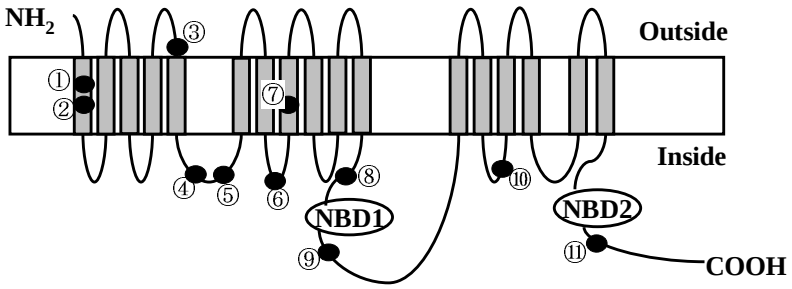


| | ① | ② | ③ | ④ | ⑤ | ⑥ | ⑦ | ⑧ | ⑨ | ⑩ | ⑪ |
|---|---|---|---|---|---|---|---|---|---|---|---|
| [AA position] | 41 | 42 | 162 | 270 | 290 | 401 | 439 | 613 | 706 | 1090 | 1502 |
| AF282772 (AKR/J) | L | L | T | T | S | K | L | R | A | D | I |
| AF282773 (C57L/J) | L | L | T | T | S | K | L | Q | A | D | I |
| AF227274 and NM_013806 (house mouse) | F | W | A | P | A | E | R | Q | S | V | V |
| Present product (BALB/c) | L | L | A | P | A | K | L | R | A | D | I |

## Monkey Mrp2

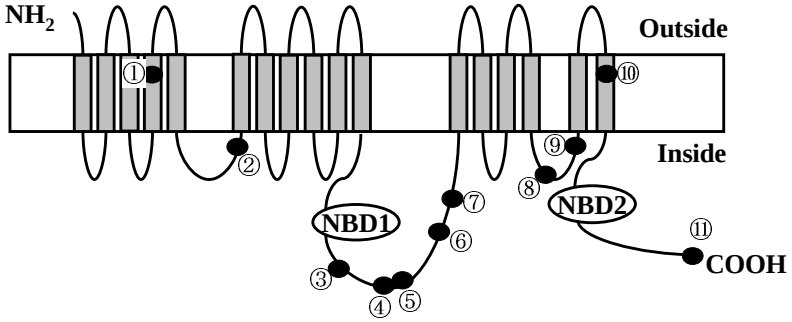


| | ① | ② | ③ | ④ | ⑤ | ⑥ | ⑦ | ⑧ | ⑨ | ⑩ | ⑪ |
|---|---|---|---|---|---|---|---|---|---|---|---|
| [AA position] | 152 | 292 | 698 | 745 | 746 | 898 | 921 | 1166 | 1202 | 1234 | (C-term) |
| DQ015923 (Macaca mulatta) | W | I | R | T | R | A | S | T | T | N | STEL |
| AF410948 and NM_001032847 (Macaca mulatta) | W | I | R | T | R | P | S | A | T | N | S-IL |
| Present product (Macaca fascicularis) | R | T | K | M | L | A | G | T | I | S | S-IL |

DMD Fast Forward. Published on August 25, 2006 as DOI: 10.1124/dmd.106.010991
This article has not been copyedited and formatted. The final version may differ from this version.

Fig. 2

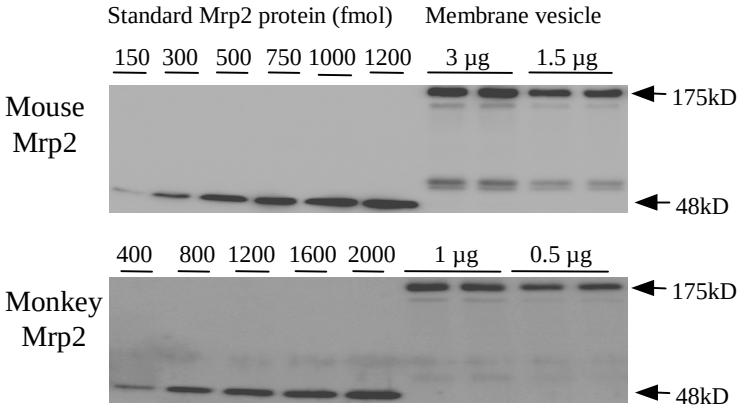

DMD Fast Forward. Published on August 25, 2006 as DOI: 10.1124/dmd.106.010991
This article has not been copyedited and formatted. The final version may differ from this version.

Fig. 3

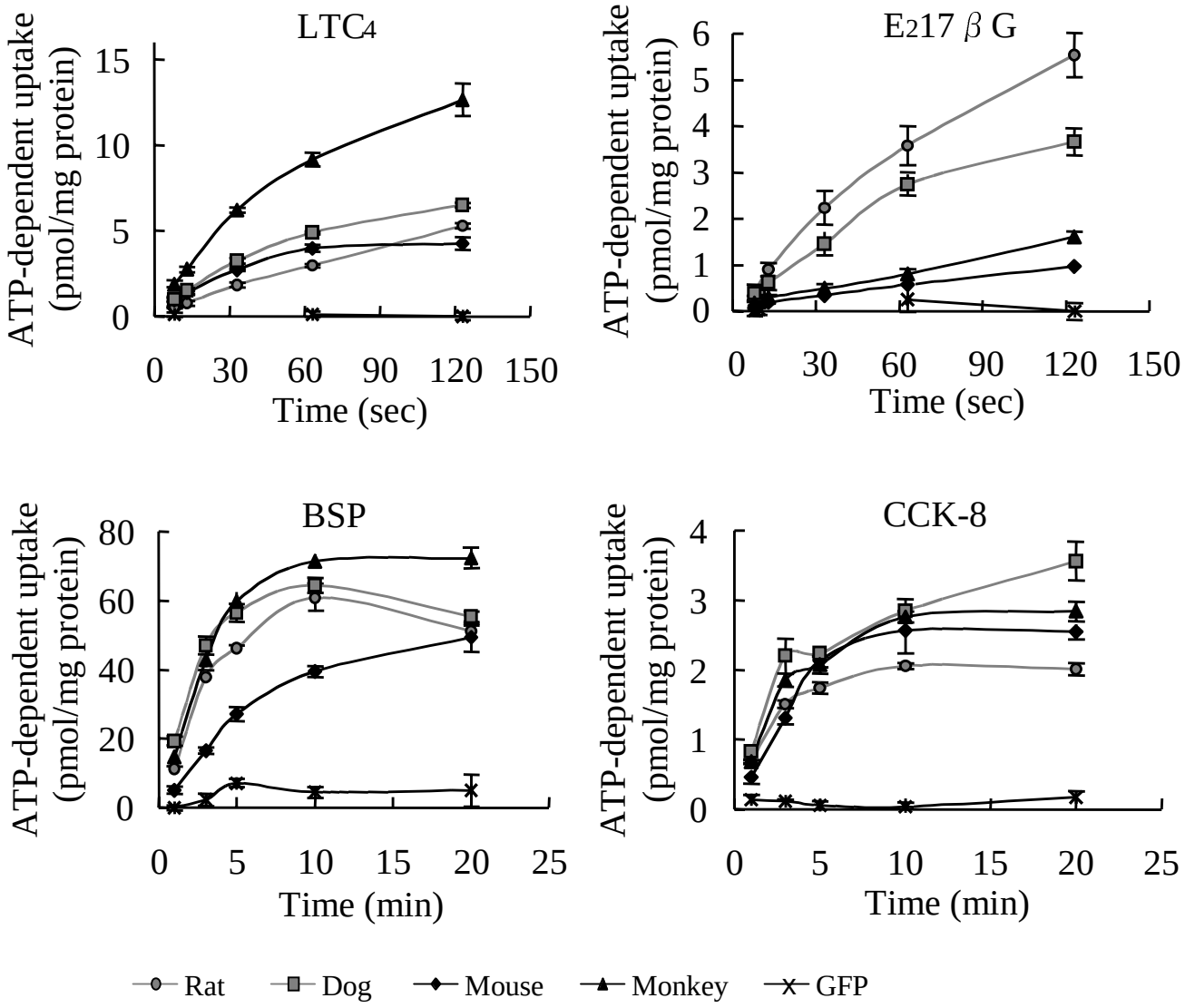

DMD Fast Forward. Published on August 25, 2006 as DOI: 10.1124/dmd.106.010991
This article has not been copyedited and formatted. The final version may differ from this version.

Fig. 4

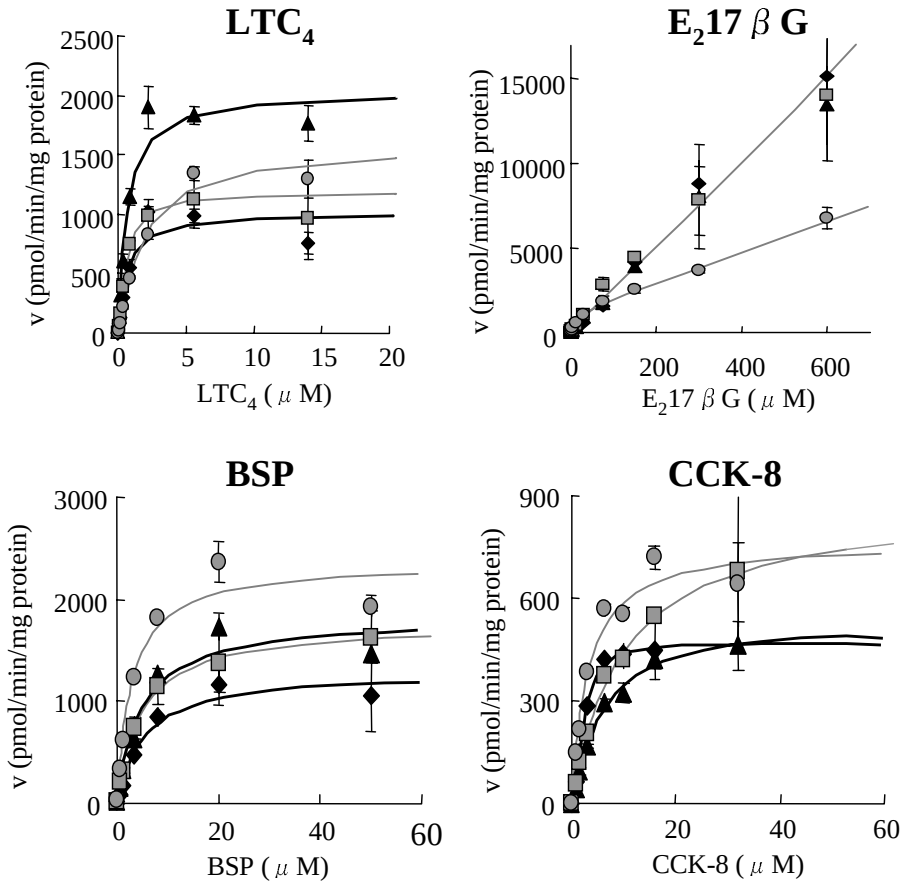

DMD Fast Forward. Published on August 25, 2006 as DOI: 10.1124/dmd.106.010991
This article has not been copyedited and formatted. The final version may differ from this version.

Fig. 5

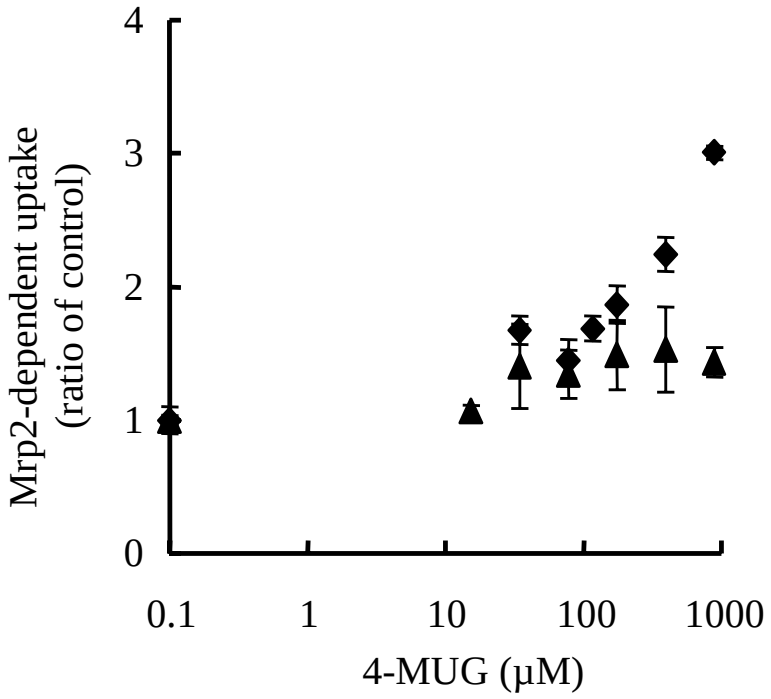

DMD Fast Forward. Published on August 25, 2006 as DOI: 10.1124/dmd.106.010991
This article has not been copyedited and formatted. The final version may differ from this version.

Fig. 6